CHAPTER VI
METAL ION ADSORPTION IN COLUMN EXPERIMENT

6.1 Single-species metal ion adsorption in column experiment

6.1.1 Effect of bed depth

The operation of a fixed bed adsorber is dependent on a large extent on the shape of the curve given by plotting C/C_0 versus time or volume. This curve is referred to as a breakthrough curve. The breakthrough curves obtained from the adsorption of Cu(II) and Pb(II) each at 0.3 mmol l^{-1} initial concentrations at different bed depths (1.5, 3.0 and 4.5 cm) for a constant linear flow rate of 2.5 ml min^{-1} are shown in Figure 6.1. The bed capacity and the percent removal of both Cu(II) and Pb(II) increased with increasing bed height (Table 6.1), as more binding sites were available for sorption. The breakthrough time (t_b) and exhaustion time (t_x) increased with an increase in bed height. This character is illustrated in Figure 6.1 where the sorbent in longer columns could be employed more effectively than those in shorter columns. The same figure illustrates that, as the bed height increased, metal had more time to contact with activated carbon and also the column provided more binding sites for the metal, and these resulted in higher metal removal efficiency. Thus, the column with longer bed depth could uptake more metal resulting in a decrease in the solute concentration in the effluent.

The influence of bed height on the sorption efficiency could be indicated using the concept of the number of transfer unit (NTU) which was defined as the ratio between the total bed depth (D) to the length of mass transfer zone (Z) (Namane and Hellal, 2006). Generally, the mass transfer zone (MTZ) is the area within the adsorption column where adsorbate is actually being adsorbed on the adsorbent (Figure 6.2). The length of the mass transfer zone (Z) can be estimated from the breakthrough curve data (Volesky et al., 2003):

$$Z = D\left(1 - \frac{t_b}{t_x}\right) \qquad (6.1)$$

where D is the total bed depth (cm), t_b breakthrough time (min), t_x bed exhaustion time (min).
The MTZ typically moves from the influent end toward the effluent end of the adsorption column during operation. In other words, the adsorbent near the influent is utilized initially and once it becomes saturated (spent) with adsorbate, the zone of active adsorption moves toward the effluent end of the bed where the adsorbent is not yet saturated. Table 6.2 demonstrates the

length of the mass transfer zone at various column lengths. As adsorption capacity is used up in each zone, the MTZ advances down the bed until the adsorbate begins to appear in the effluent. The concentration gradually increases until it equals the influent concentration. The length of the mass transfer zone could be used to calculate the number of mass transfer zone (or the number of transfer unit) which would then explain the efficiency of the column (Namane and Hellal, 2006). The calculation of the number of transfer unit is giving by the ratio:

$$\text{Number of the transfer unit (NTU)} = D / Z \qquad (6.2)$$

where D is the total bed depth (cm), Z the length of mass transfer zone.

Table 6.2 shows the number of transfer unit at various column lengths. The result shows that NTU of Cu(II) was equal to 1.33 for the bed depth of 1.5 cm, 2.67 for 3.0 cm, and 6.00 for the bed depth of 4.5 cm, at a constant flow rate of 2.5 ml min^{-1}. The NTU of Pb(II) was equal to 1.25 for the bed depth of 1.5 cm, 3.00 for 3.0 cm, and 7.50 for the bed depth of 4.5 cm, at a constant flow rate of 2.5 ml min^{-1}. In both cases, the maximum NTU occurred at the bed depth of 4.5 cm. This was interesting as an increase in NTU seemed to occur at a faster rate than an increase in the bed depth. For instance, as the bed doubled its depth, NTU became higher but much more than double the original value. This was because the entrance/exit effect. For short columns, the entrance/exit effect was significant and the column would have to be prematurely regenerated. For long columns, the entrance/exit effect became less significant and therefore the column could be employed more efficiently. Table 6.2 also demonstrates that, generally, Pb(II) had more NTU than Cu(II). This implied that eucalyptus bark could remove of Pb(II) better than Cu(II).

6.1.2 Effect of flow rate

For this experiment, the flow rate was varied from 2.5 to 7.5 ml min^{-1} while the inlet Cu(II) and Pb(II) concentrations in the feed were held constant at 0.3 mg l^{-1} and the bed depth of 1.5 cm. The plots of Cu(II) and Pb(II) concentration versus time at different flow rates are given in Figure 6.3. The total uptake quantity (m_{total}), equilibrium uptake q_{column} and the total removal percentage with respect to flow rate were evaluated from the sorption data and are presented in Table 6.1. As the adsorption zone moves down and the upper edge of this zone reaches the bottom of the column, the effluent concentration starts to rise rapidly (Faust and Aly, 1987). It is observed that the breakthrough curve becomes steeper when the flow rate was increased with

which the break point time and adsorbed metal ion concentration decreases. On the other hand, if the liquid flowed more slowly, metal had more time to contact with activated carbon resulting in a better metal removal in the column. Hence, a decrease in the metal removal percentage was observed with an increase in flow rate: at 2.5 ml min^{-1}, 29.7% of Cu(II) and 40.2 % of Pb(II) could be reached, and this was decreased to 28.3% of Cu(II) and 37.5% of Pb(II) at 5.0 ml min^{-1} and the bed depth of 1.5 cm. A further decrease in flow rate to 7.5 ml min^{-1} and the bed depth of 1.5 cm saw a decrease in the adsorptions of Cu(II) and Pb(II) to 27.6 and 34.2%, respectively.

Table 6.2 demonstrates the relationship between the NTU and the flowrate which demonstrated that the NTU generally decreased with an increase in the flowrate. This was because a faster liquid flow required a longer time to reach equilibrium and therefore increased the length of the MTZ. For instance, the number of transfer unit of Cu(II) was equal to 1.33 at flow rate of 2.5 ml min^{-1}, 0.51 at flow rate of 5.0 ml min^{-1}, and 0.34 at flow rate of 7.5 ml min^{-1}, at a constant bed depth of 1.5 cm.

6.1.3 Experiment VS Thomas model

A mathematical model based on mass balance is often used to explain the adsorption column characteristics. Various kinetic models have been developed to express the dynamic behavior of the column. The Thomas equation is one of the most general and widely used models to predict the adsorption characteristics and this can be expressed as (Thomas, 1994):

$$\frac{C}{C_0} = \frac{1}{1000 + \exp\left[k_{Th} / Q(q_{Th} X - C_0 V_{eff})\right]} \tag{6.3}$$

where k_{Th} is the Thomas rate constant (ml min^{-1} $mmol^{-1}$), q_{Th} the equilibrium metal uptake per gram of the adsorbent (mmol g^{-1}), X amount of adsorbent in the column (g), V_{eff} effluent volume (ml), C_0 initial metal ions concentration (mmol l^{-1}), C the effluent metal ions concentration (mmol l^{-1}), and Q flow rate (ml min^{-1}). The linearized form of the Thomas model is as follows:

$$\ln\left(\frac{C}{C_0} - 1\right) = \frac{k_{Th} q_{Th} X}{Q} - \frac{k_{Th} C_0}{Q} V_{eff} \tag{6.4}$$

The kinetic coefficient k_{Th} and the adsorption capacity of the column q_{Th} can be determined from a plot of $\ln(C_0/C-1)$ against V_{eff} at a given flow rate with a slope of $(-k_{Th}C_0/Q)$ and an intercept of $(k_{Th}q_oX/Q)$. The fitting results are displayed in Table 6.3 where the high R^2 indicated that the experimental results could fit with the Thomas model using linear regressive coefficients, and

therefore this model could be used with certain level of confidence to describe the adsorption column.

The relative parameters are listed in Table 6.3 which illustrates that the values of k_{Th} increased with increasing of flow rate. The Thomas rate constant k_{Th} became smaller for the systems with higher adsorption capacity because it took longer for saturation to be reached in these cases (Aksu and Gönen, 2004). It was also shown that the Thomas rate constant increased as the flow rate increased, and this indicated that the adsorption would reach equilibrium faster at this condition.

6.1.4 Experiment VS the bed depth-service-time model (BDST)

One of the simplest models used to describe the adsorption column is the bed depth-service-time model (BDST), which was based on Bohart and Adams theory (Bohart and Adams, 1920). This model assumes that the rate of adsorption is controlled by the surface reaction between the adsorbate and the unused capacity of the solid. The most important criterion in the design of fixed bed sorption systems is the prediction of fixed bed column breakthrough or the shape of the sorption wave front, which determines the operation life span of the bed. The BDST model gives a linear relationship between the time required to reach the desired breakthrough concentration (t_b) and the bed depth (D) that is:

$$t_b = \frac{N_0 D}{C_0 V} - \frac{1}{K C_0} \ln\left(\frac{C_0}{C_b} - 1\right) \tag{6.5}$$

where N_0 is the initial adsorptive capacity per unit volume of bed (mmol l^{-1}), C_0 the bed influent concentration (mmol l^{-1}), C_b the desired concentration of solute at breakthrough, K the adsorption rate constant (ml $mmol^{-1}$ min^{-1}), D the bed depth of column (cm), V the linear flow velocity of feed to bed (ml min^{-1}), t is the service time of column under above conditions (min).

The Bohart–Adams Eq. (6.5) can be expressed in a simple linear form as:

$$t = aD + b \tag{6.6}$$

where

$$a = slope = \frac{N_0}{C_0 V} \tag{6.7}$$

and

$$b = \text{intercept} = -\frac{1}{KC_0}\ln\left(\frac{C_0}{C_b} - 1\right) \qquad (6.8)$$

The plots of service time, t_b, versus bed depth, D, for the sorption of Cu(II) and Pb(II) are shown in Figure 6.4. The initial concentration, Co, and the flow velocity, V, were assumed to be reasonably constant during the column operation. The values of K and N_0 calculated from the slope and intercept of the linear plot are presented in Table 6.4. From the table, it is evident that the maximum sorption capacity (N_0) decreased with an increase in flow rate. These results correlate well with the observed sorption capacity and showed poor adsorber performance at high flow rate. As the flow rate increased, the effluent volume required for complete column saturation decreased for both sorbents due to less interaction between the metal ion and sorbent (as described earlier). Therefore, the higher bed column resulted in a decrease in the metal concentration in the effluent. The sorption rate constant (K) characterizes the rate of solute transfer from liquid to solid phases (Vijayaraghavan, et al., 2005). The values of the sorption rate constant (K) were influenced by flow rate and increased with an increase in flow rate. Figure 6.4 illustrates that the variation of the service time with bed depth was relatively linear, thus indicating the validity of the BDST model when applied to the continuous column studies. The BDST model parameters can be helpful to scale up the process to minimize the experimental runs.

The form of the Bohart–Adams equation, shown in Eq. (6.9), can be used to determine the service time, t, of a column of bed depth, D, given the values of N_0, C_0 and K, which must be determined from experiments operated over a range of velocity values, V. Setting $t = 0$ and solving Eq. (6.5) for D yields

$$D_0 = \frac{V}{KN_0}\ln\left(\frac{C_0}{C_b} - 1\right) \qquad (6.9)$$

where D_0 is the critical bed depth necessary to produce an effluent concentration C_b, also known as critical bed depth.

The critical bed depth (D_0) is the theoretical depth of the sorbent sufficient to prevent the adsorbate concentration from exceeding C_b (breakthrough concentration) at $t = 0$. The results in Table 6.4 show that D_0 was higher at higher flow rate because the adsorption zone or MTZ must be increased to remove the metal under the higher flow rate. The sorption capacity of Pb(II) was higher than that of Cu(I) for all flow rates and bed heights used in this study.

6.2 Binary-species metal ion adsorption in column experiment

The adsorption of a single metal is not a common process in industries. Wastewater effluent normally contains multi-species metals with various concentrations and flow rates. However, adsorption capacities and rates of adsorption may alter upon adsorption of mixtures of metals. From the single adsorption experiment, for Cu(II) and Pb(II) at 0.3 mmol l^{-1}, the optimum bed depth was 4.5 cm at the flow rate of 2.5 ml min^{-1} where the adsorption capacities of Cu(II) and Pb(II) were 0.199 and 0.216 mmol g^{-1}, respectively. This condition was selected for the study of binary component (Cu-Pb) in adsorption column experiments. However, the adsorption performance of the binary-metal solutions was tested using the solution with equal initial concentration of 0.15 mmol l^{-1}. The results of these experiments are shown in Table 6.5. The breakthrough curves for Cu(Cu-Pb) and Pb(Cu-Pb) removal from a binary-species system using activated carbon are shown in Figure 6.4. This indicated that the carbon tended to adsorb Pb(Cu-Pb) better than Cu(Cu-Pb). However, Pb(Cu-Pb) may need more time to reach exhaustion, i.e. the breakthrough for Pb(II) occurred at around 60 min (Figure 6.5) while that of Cu(II) occurred at a much earlier time (30 min). It is illustrated that the adsorption capacity of Cu(Cu-Pb) also decreased as Pb(Cu-Pb) was added. This suggested that the function groups on the surface of activated carbon had a relatively stronger affinity for Pb(Cu-Pb) ions than Cu(Cu-Pb) ions. To confirm this conclusion, the value of k_{Th} of Pb(Cu-Pb) was also found to be higher than that of Cu(Cu-Pb) under the same conditions. The parameters of q_{Th} and k_{Th} in the Thomas model are listed in Table 6.5. The comparison between Table 6.5 and Table 6.3 suggested that the adsorption capacity in the binary system was lower than that in the single metal systems. Table 6.5 shows that the length of MTZ for Cu(Cu-Pb) was 1.25 which was higher than that of Pb(Cu-Pb) which was 1.14, this also concludes the stronger adsorption for Pb(II) over Cu(II). A comparison of the experimental sorption capacities and the predicted values obtained from the Thomas model (q_{Th}) demonstrates that the calculated q_{column} was significantly closer to the experimental q_{column}. Hence, it was concluded that the adsorption here could be better represented by Thomas model.

The result from the binary components adsorption were compared with those obtained from the single component adsorption which was performed in the column with the bed depth of 4.5 cm, the flow rates at 2.5 ml min^{-1} and on equal molar concentration of 0.3 mmol L^{-1} (molar basis). The results as given in Table 6.6 revealed that, in the equimolar concentration of heavy

metal, the single component adsorption had higher adsorption than the binary component adsorption. Values of the column uptake capacities q_{Th} obtained from the Thomas model for the binary-component system at described conditions were 0.026 and 0.030 mmol g^{-1} for Cu(Cu-Pb) and Pb(Cu-Pb), respectively. The adsorption order for Cu(Cu-Pb) and Pb(Cu-Pb) ions in the binary-component system is Pb(II) > Cu(II) which was the same as that obtained from the single component. This observation is in agreement with that reported by other studies (Mckenzie, 1980).

6.3 Concluding remarks

The performance of the activated carbon for the removal of metal under dynamic conditions was studied. The useful parameters for the future design of the sorption column such as the BDST parameters and the Thomas model parameters were also determined. The column design parameters as obtained could be used for the design of adsorption column in practical applications. Results from the model can be used in the scale up and in the prediction of the performance of full-scale treatment systems. By comparing the results of this study to the previous batch experiment, it was found that the fixed-bed columns tended to reduce the treatment efficiencies of the adsorbents, possibly as a result of the reduced contact time in the columns which may not have been adequate to reach adsorption equilibrium.

Table 6.1 Effects of flow rate and bed depth on the total uptake quanity (m_{total}), equilibrium uptake (q_{column}) and the total removal percentage

Metal	Flow rate (ml min^{-1})	Bed depth (cm)	t_{total} (min)	V_{eff} (ml)	m_{total} (mmol)	q_{total} (mmol)	q_{column} (mmol g^{-1})	Total metal removal (%)
	2.5	1.5	360	900	0.268	0.080	0.159	29.7
	5.0	1.5	150	750	0.212	0.066	0.132	28.3
	7.5	1.5	60	450	0.127	0.035	0.070	27.6
	2.5	3.0	480	1200	0.334	0.174	0.174	52.1
Cu(II)	5.0	3.0	210	1050	0.292	0.154	0.154	52.8
	7.5	3.0	90	675	0.193	0.101	0.101	52.4
	2.5	4.5	540	1350	0.389	0.284	0.190	73.0
	5.0	4.5	240	1200	0.340	0.232	0.155	68.4
	7.5	4.5	120	900	0.255	0.143	0.095	56.1
	2.5	1.5	450	1125	0.304	0.122	0.244	40.2
	5.0	1.5	210	1050	0.280	0.105	0.210	37.5
	7.5	1.5	90	675	0.140	0.048	0.096	34.2
	2.5	3.0	540	1350	0.401	0.253	0.253	62.9
Pb(II)	5.0	3.0	240	1200	0.347	0.217	0.217	62.4
	7.5	3.0	120	900	0.252	0.129	0.129	51.2
	2.5	4.5	600	1500	0.437	0.412	0.275	94.4
	5.0	4.5	270	1350	0.387	0.333	0.222	86.2
	7.5	4.5	150	1125	0.312	0.161	0.107	51.6

Table 6.2 Length of mass transfer zone (Z) and the number of transfer unit (D/Z) at various column lengths and flow rates

Metal	Flow rate (ml min^{-1})	Bed depth (cm)	Z (cm)	Number of transfer unit (-)
Cu(II)	2.5	1.5	1.13	1.33
	5.0	1.5	2.94	0.51
	7.5	1.5	4.43	0.34
	2.5	3.0	1.13	2.67
	5.0	3.0	2.79	1.08
	7.5	3.0	4.05	0.74
	2.5	4.5	0.75	6.00
	5.0	4.5	2.63	1.71
	7.5	4.5	3.94	1.14
Pb(II)	2.5	1.5	1.20	1.25
	5.0	1.5	2.79	0.54
	7.5	1.5	4.05	0.35
	2.5	3.0	1.00	3.00
	5.0	3.0	2.63	1.14
	7.5	3.0	3.94	0.76
	2.5	4.5	0.60	7.50
	5.0	4.5	2.33	1.93
	7.5	4.5	3.60	1.25

Table 6.3 Parameters predicted from Thomas model at different flow rates and bed depths

Metal	Flow rate (ml min^{-1})	Bed depth (cm)	q_{Th} (mmol g^{-1})	k_{Th} (l min^{-1} $mmol^{-1}$)	R^2
Cu(II)	2.5	1.5	0.153	0.081	0.9808
	5.0	1.5	0.120	0.293	0.9539
	7.5	1.5	0.057	0.425	0.9919
	2.5	3.0	0.161	0.082	0.9540
	5.0	3.0	0.152	0.214	0.9714
	7.5	3.0	0.083	0.228	0.9845
	2.5	4.5	0.199	0.083	0.9987
	5.0	4.5	0.140	0.085	0.9553
	7.5	4.5	0.091	0.143	0.9522
Pb(II)	2.5	1.5	0.235	0.115	0.9960
	5.0	1.5	0.196	0.131	0.8897
	7.5	1.5	0.087	0.352	0.9701
	2.5	3.0	0.244	0.056	0.9903
	5.0	3.0	0.215	0.099	0.8651
	7.5	3.0	0.123	0.112	0.9948
	2.5	4.5	0.267	0.040	0.9832
	5.0	4.5	0.164	0.048	0.9830
	7.5	4.5	0.107	0.235	0.9948

Table 6.4 BDST model parameters for sorption of Cu and Pb ions at different bed depths and flow rates

Metal	Flow rate (ml min^{-1})	D_o (cm)	N_o (mmol l^{-1})	K (l $mmol^{-1}$ min^{-1})	R^2
Cu(II)	2.5	0.33	25.20	0.37	0.8710
	5.0	1.22	7.56	0.67	0.9959
	7.5	1.21	5.88	1.29	0.9932
Pb(II)	2.5	0.29	29.40	0.37	0.9932
	5.0	0.67	12.60	0.73	0.9643
	7.5	0.43	8.82	2.44	0.9423

Table 6.5 Adsorption of Cu(Cu-Pb) and Pb(Cu-Pb) for the adsorption at flow rates of 2.5 ml min^{-1} at influent concentration of 0.15 mmol l^{-1} and bed depth of 4.5 cm

Parameter	Metal	
	Cu(Cu-Pb)	Pb(Cu-Pb)
t_{total} (min)	180	210
V_{eff} (ml)	450	525
m_{total} (mmol)	0.062	0.074
q_{total} (mmol)	0.033	0.046
q_{column} (mmol g^{-1})	0.022	0.031
Total metal removal (%)	53.2	62.3
Z (cm)	1.25	1.14
NTU	3.60	3.95
k_{Th} (l min^{-1} $mmol^{-1}$)	0.221	0.240
q_{Th} (mmol g^{-1})	0.026	0.030
R^2	0.9724	0.9955

Table 6.6 Comparison between adsorption from single and binary adsorption

Parameter	Single species		binary species	
	Cu	Pb	Cu(Cu-Pb)	Pb(Cu-Pb)
t_{total} (min)	540	600	180	210
V_{eff} (ml)	1350	1500	450	525
m_{total} (mmol)	0.389	0.437	0.062	0.074
q_{total} (mmol)	0.284	0.412	0.033	0.046
q_{column} (mmol g^{-1})	0.190	0.275	0.022	0.031
Total metal removal (%)	73.0	94.4	53.2	62.3
Z (cm)	0.75	0.60	1.25	1.14
NTU	6.00	7.50	3.60	3.95
k_{Th} (l min^{-1} $mmol^{-1}$)	0.083	0.040	0.221	0.240
q_{Th} (mmol g^{-1})	0.199	0.276	0.026	0.030
R^2	0.9987	0.9832	0.9724	0.9955

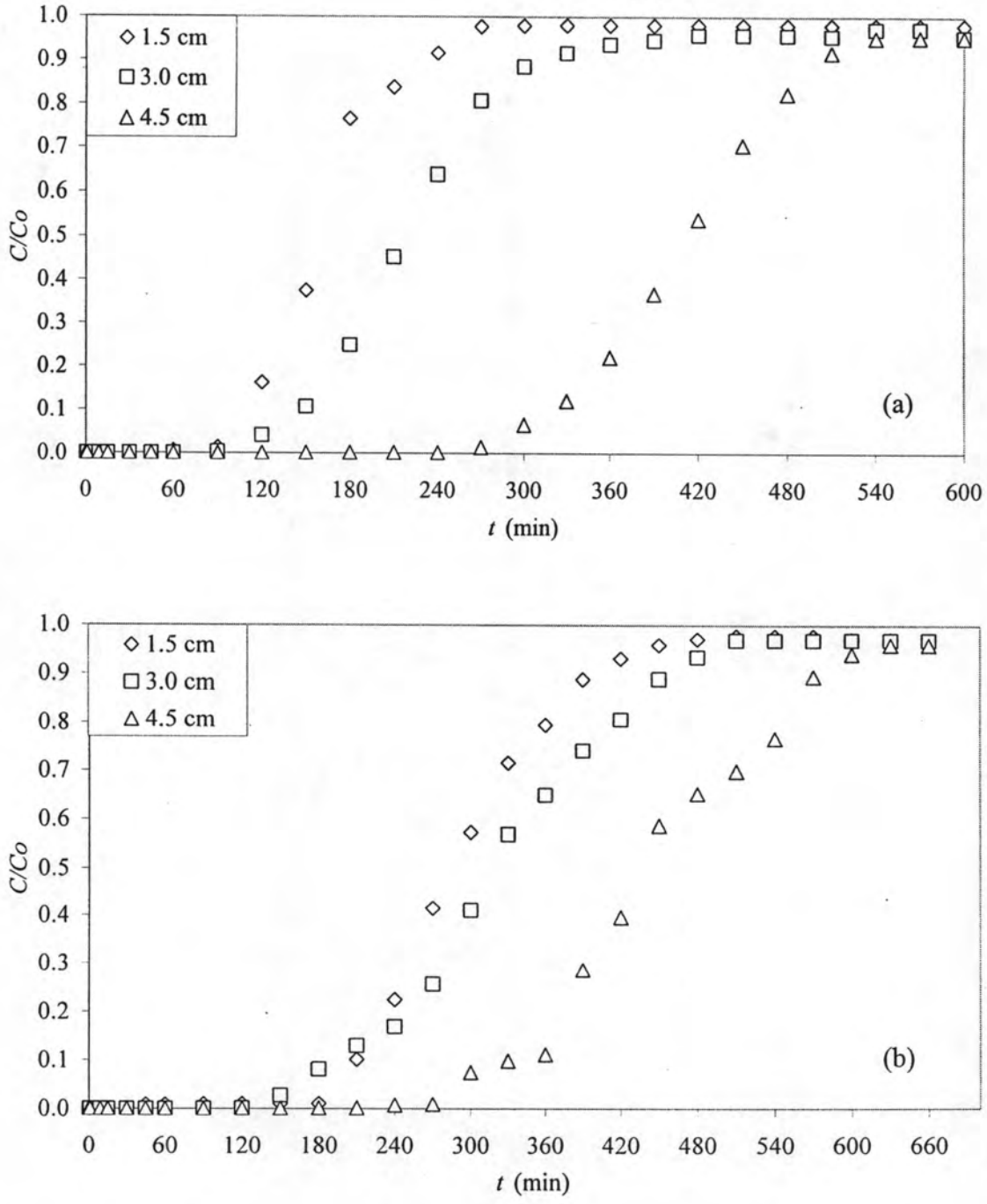

Figure 6.1 Breakthrough curves of (a) Cu(II) and (b) Pb(II) for the adsorption at different bed depths at influent concentration of 0.3 mmol l^{-1} and liquid flow rate of 2.5 ml min^{-1}.

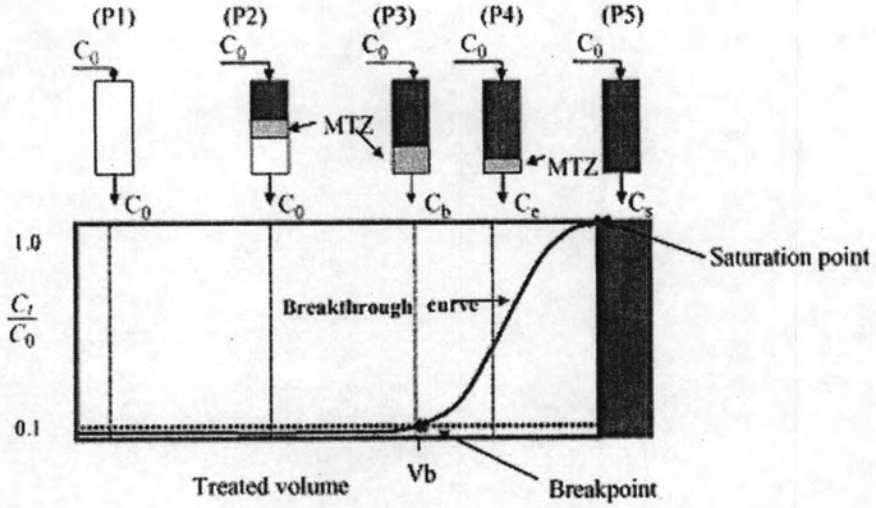

Figure 6.2 Typical breakthrough curve for activated carbon showing the movement of the mass transfer zone according to the throughput volume.

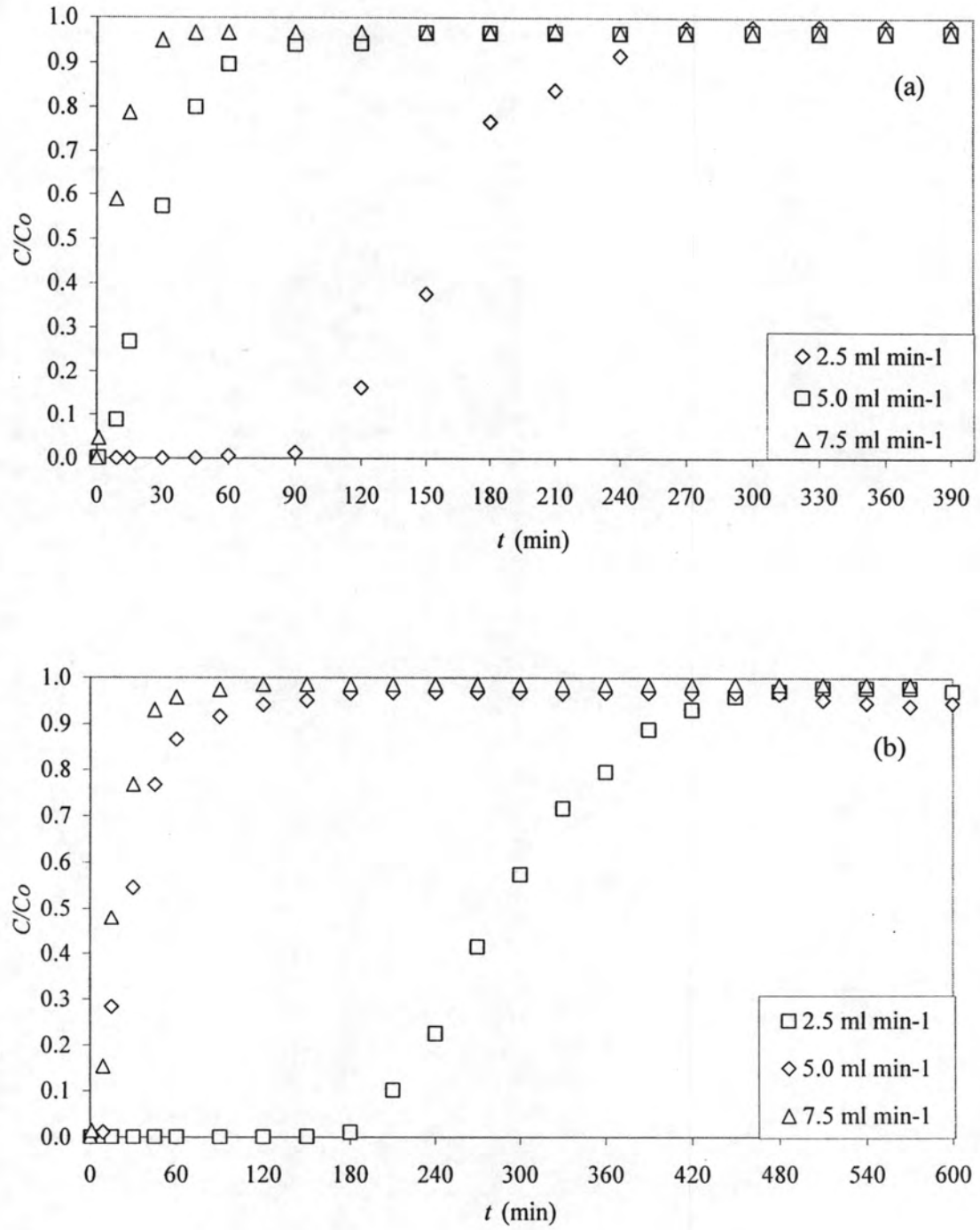

Figure 6.3 Breakthrough curves of (a) Cu(II) and (b) Pb(II) for the adsorption at different flow rates at influent concentration of 0.3 mmol l^{-1} and bed depth of 1.5 cm.

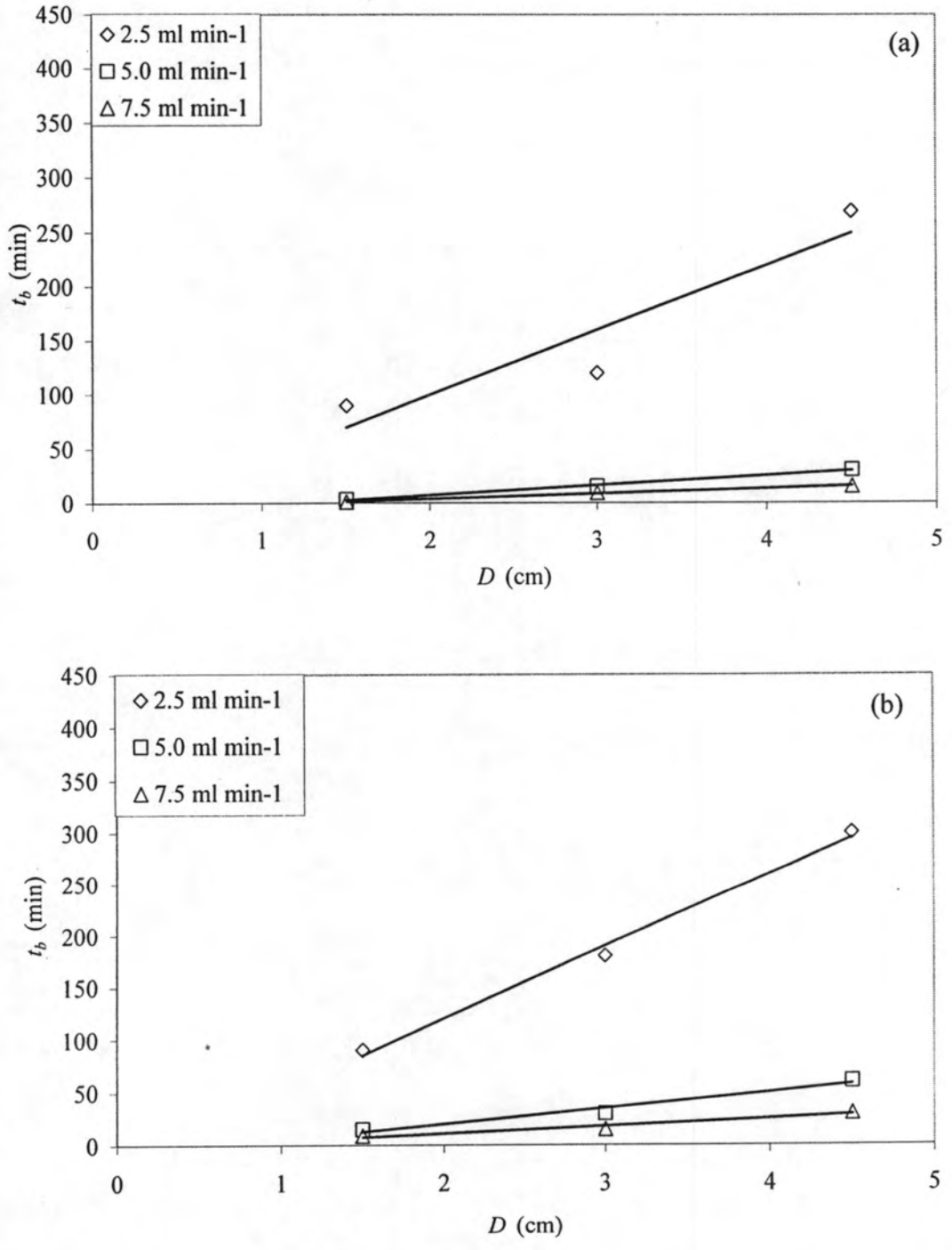

Figure 6.4 BDST model plot for Cu(II) (a) and Pb(II) (b) at different flow rates at influent concentration of 0.3 mmol l^{-1}

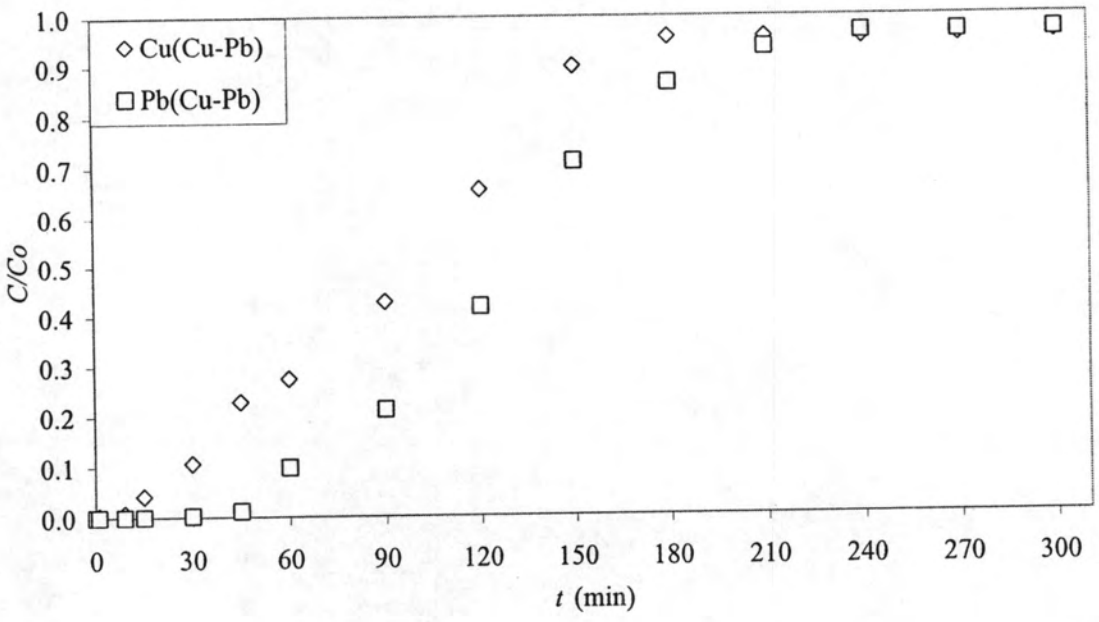

Figure 6.5 Breakthrough curves of (a) Cu(Cu-Pb) and (b) Pb(Cu-Pb) for the adsorption at flow rates of 2.5 ml min^{-1}at influent concentration of 0.15 mmol l^{-1} and bed depth of 4.5 cm.